MOLECULAR AND CELLULAR BIOLOGY, Apr. 2008, p. 2358–2367 Vol. 28, No. 7
0270-7306/08/$08.00+0 doi:10.1128/MCB.01722-07

Krüppel-Like Zinc Finger Protein Glis2 Is Essential for the Maintenance of Normal Renal Functions▽†

Yong-Sik Kim,[1] Hong Soon Kang,[1] Ronald Herbert,[2] Ju Youn Beak,[1] Jennifer B. Collins,[3] Sherry F. Grissom,[3] and Anton M. Jetten[1]*

Division of Intramural Research, Cell Biology Section,[1] Laboratory of Experimental Pathology,[2] and Microarray Group,[3] National Institute of Environmental Health Sciences, National Institutes of Health, Research Triangle Park, North Carolina 27709

Received 19 September 2007/Returned for modification 22 October 2007/Accepted 20 January 2008

To obtain insight into the physiological functions of the Krüppel-like zinc finger protein Gli-similar 2 (Glis2), mice deficient in Glis2 expression were generated. Glis2 mutant ($Glis2^{mut}$) mice exhibit significantly shorter life spans than do littermate wild-type (WT) mice due to the development of progressive chronic kidney disease with features resembling nephronophthisis. $Glis2^{mut}$ mice develop severe renal atrophy involving increased cell death and basement membrane thickening in the proximal convoluted tubules. This development is accompanied by infiltration of lymphocytic inflammatory cells and interstitial/glomerular fibrosis. The severity of the fibrosis, inflammatory infiltrates, and glomerular and tubular changes progresses with age. Blood urea nitrogen and creatinine increase, and $Glis2^{mut}$ mice develop proteinuria and ultimately die prematurely of renal failure. A comparison of the gene expression profiles of kidneys from 25-day-old/60-day-old WT and $Glis2^{mut}$ mice by microarray analysis showed increased expressions of many genes involved in immune responses/inflammation and fibrosis/tissue remodeling in kidneys of $Glis2^{mut}$ mice, including several cytokines and adhesion and extracellular matrix proteins. Our data demonstrate that a deficiency in Glis2 expression leads to tubular atrophy and progressive fibrosis, similar to nephronophthisis, that ultimately results in renal failure. Our study indicates that Glis2 plays a critical role in the maintenance of normal kidney architecture and functions.

Gli-similar 1 (Glis1) through Glis3 form a subfamily of Krüppel-like zinc finger proteins that are related to members of the Gli and Zic subfamilies (1, 20, 21, 23, 24, 28, 35, 46, 47). Members of these families share a highly conserved tandem repeat of five C_2H_2-type zinc finger (ZF1 to ZF5) motifs. These zinc finger domains recognize specific DNA elements, referred to as Gli-binding sites (GBS), in the promoter regions of target genes and can regulate their transcription in a positive or negative manner (23–25, 33). Gli and Zic proteins are critical in the regulation of embryonic development and have been implicated in several disease processes, including various cancers (1, 16, 20, 32).

Relatively little is known about the physiological functions of Glis proteins. Glis1 expression was shown to be elevated in psoriatic skin (34); however, mice deficient in Glis1 did not exhibit any apparent phenotype (35). Glis3 was shown to enhance osteoblast differentiation that involves increased expression of FGF18 (3). Mutations in GLIS3 have been linked to a human syndrome consisting of neonatal diabetes and congenital hypothyroidism, suggesting that GLIS3 might have a critical role in pancreatic development (2a, 41). The overexpression of GLIS3 in ependymomas was found to be associated with a poor prognosis (31). Glis2 is expressed in several adult tissues, most abundantly in kidney (28, 46, 47). During embryonic development, Glis2 mRNA is expressed in a temporal and spatial manner. At embryonic day 11.5 of mouse embryonic development, Glis2 is most highly expressed in the ureteric bud (the inductor of the mesenchymal-epithelial conversion) and, in adult kidney, in tubules and collecting ducts. A recent study linked the loss of GLIS2 function to nephronophthisis, an autosomal recessive kidney disease and the most frequent genetic cause for end-stage renal failure (2). It is characterized by renal fibrosis and tubular atrophy, resulting in the loss of renal tissue architecture (14). Glis2 is also expressed in the cranial and dorsal ganglia, the neural tube, and in the intermediate zones of the hindbrains of mouse embryos (embryonic day 9.5) (47). Exogenous expression of Glis2 has been reported to promote the differentiation of neuronal precursor cells, suggesting a regulatory role of Glis2 in neuronal differentiation (28). The precise physiological functions of Glis2 need to be established.

To obtain greater insight into the physiological functions of Glis2, we generated mice deficient in the expression of Glis2 ($Glis2^{mut}$). Our data demonstrate that $Glis2^{mut}$ mice develop progressive kidney disease that is associated with tubular atrophy through apoptosis, severe inflammation, and fibrosis that ultimately results in renal failure. Gene expression profile analysis showed increased expression of many genes involved in a variety of proinflammatory and profibrotic responses. Our observations are in agreement with the results of a recent study showing that deficiency in GLIS2 expression leads to progressive chronic kidney disease similar to nephronophthisis (2). These studies indicate that Glis2 is critical for the maintenance

* Corresponding author. Mailing address: Division of Intramural Research, Cell Biology Section, National Institute of Environmental Health Sciences, National Institutes of Health, Research Triangle Park, NC 27709. Phone: (919) 541-2768. Fax: (919) 541-4133. E-mail: jetten@niehs.nih.gov.

† Supplemental material for this article may be found at http://mcb.asm.org/.

▽ Published ahead of print on 28 January 2008.

of the normal renal architecture and functions. The Glis2^{mut} mice will provide an excellent model to study the molecular events that play a role in the initiation and progression of nephronophthisis.

MATERIALS AND METHODS

Generation of Glis2^{mut} mice. The pOSdupdel-Glis2 targeting vector was designed to replace a 1.5-kb region that includes exon 6 by a 1.8-kb neomycin cassette containing the phosphoglycerate kinase poly(A)$^+$ signal and the neomycin phosphotransferase (neo) selectable marker under the control of a phosphoglycerate kinase promoter. The genomic flanking regions were generated by PCR amplification using 129Sv genomic DNA as a template. The 6-kb BclI/ClaI fragment included exons 1 through 5 and the 2-kb Kpn1/NotI fragment contained the flanking region downstream of the Glis2 gene. pOSdupdel-Glis2 was linearized by NotI and electroporated into E14Tg2a embryonic stem (ES) cells that were derived from mouse strain 129HsdOla. G418-resistant ES clones were isolated and screened by Southern blot analysis for homologous recombination events by using both 5′ and 3′ probes. Gene-targeted ES cells were microinjected into blastocysts from C57BL/6 mice that were then implanted into pseudopregnant CD1 females. Offspring demonstrating agouti coat color were analyzed for the presence of the disrupted Glis2 gene. The chimeric mice were crossed with C57BL/6 mice to identify transmitting chimeras and to obtain mice heterozygous for the mutant allele. Heterozygous mice were intercrossed to obtain animals homozygous for the mutant allele and to obtain wild-type (WT) littermate controls. This gene knockout was performed at the University of North Carolina (UNC) Transgenic Facility headed by Randy Thresher. Routine genotyping was carried out by PCR. Mice were *Helicobacter* free. All animal studies followed guidelines outlined by the NIH (35a), and protocols were approved by the Institutional Animal Care and Use Committee at the National Institute of Environmental Health Services (NIEHS) and UNC.

Histopathological evaluation. Tissues were fixed in 10% neutral buffered formalin for 24 h and then transferred to 70% ethanol, processed, embedded in paraffin, sectioned at 5 microns, and stained with hematoxylin and eosin (H&E) or Masson's trichrome. Histopathological evaluation was performed on sections of tissues from male and female WT and Glis2^{mut} mice between the ages of 10 days and 12 months.

Microarray analysis. Total RNA was isolated from kidneys of 25- and 60-day-old WT and Glis2^{mut} mice by using the Qiagen RNeasy mini kit. Equal amounts of total RNA from kidneys from three individual mice were pooled. RNA from two independent experiments was used, and each microarray analysis was performed in duplicate. Gene expression analyses were conducted by the NIEHS Microarray Group on Agilent whole-mouse genome microarrays (Agilent Technologies, Palo Alto, CA). The complete listing of all the changes in gene expression in kidneys of Glis2^{mut} mice as well as the raw data are available in the supplemental material and are accessible through GEO Series accession number GSE8454.

Molecular and biochemical analysis. Western and Northern blot analyses were performed as described previously (19). Subcellular localization by confocal microscopy and reporter gene assays were carried out as reported previously (21, 24). Blood urea nitrogen (BUN) and creatinine levels and proteinuria were analyzed by standard methods, as described in the supplemental material.

Real-time QRT-PCR analyses. Total RNA isolated from kidneys was reversed transcribed using a high-capacity cDNA archive kit according to the manufacturer's instructions (Applied Biosystems). Quantitative reverse transcription-PCRs (QRT-PCRs) with 50 ng of cDNA were carried out in triplicate in a 7300 real-time PCR system (Applied Biosystems) by using the TaqMan 2× PCR Master mix and RT^2 real-time SYBR green/Rox PCR master mix (SuperArray) and the following cycles: 2 min at 50°C, 10 min at 95°C and then 40 cycles each at 95°C for 15 s and 60°C for 60 s (19). All results were normalized to an internal control, the 18S transcript. QRT-PCR analysis was also carried out using GAPDH (glyceraldehyde-3-phosphate dehydrogenase) as a control. These data confirmed the results obtained with 18S as a control. Sequences of primers used are listed in Table S1 in the supplemental material.

RESULTS

Generation of Glis2^{mut} mice. Glis2 regulates transcription by binding GBS in the regulatory regions of target genes. This binding is dependent on the 4th and 5th zinc finger motifs. To investigate the biological role of Glis2 in vivo, we generated mice in which the Glis2 gene was disrupted. We selected a strategy that would result in the deletion of the entire exon 6 region, encoding the 4th and 5th zinc fingers and the remaining carboxyl terminus of Glis2. One could predict that this deletion would impair this Glis2 function. A schematic representation of the strategy is shown in Fig. 1A. The targeting vector was created such that after homologous recombination, the 1.8-kb neomycin cassette would replace part of intron 5 and the entire exon 6 region. The disrupted Glis2 allele was ultimately transmitted through the germ line (see Fig. S1 in the supplemental material). This result was confirmed by Northern blot analysis. The 3′ Glis2 probe hybridized to the 3.5-kb Glis2 transcript of RNA isolated from kidneys of WT mice, while it did not yield any signal with RNA from Glis2^{mut} mice, thereby confirming the disruption of the Glis2 gene; however, the 5′ end of the Glis2 mRNA was still expressed in Glis2^{mut} mice (Fig. 1B). Because of the lack of a good anti-Glis2 antibody, we were unable to determine whether a truncated Glis2 protein was detectable in Glis2^{mut} mice or whether such a protein was rapidly degraded by the proteasome system.

Analysis of Glis2^{mut} activity in HEK293 cells. Glis and Gli proteins regulate transcription by binding to specific DNA binding sites (GBS) in the promoter regions of target genes (2a, 24, 25, 33, 47). ZF4 and ZF5 are essential for the binding of Gli and Glis proteins to GBS and important for the nuclear localization of Glis proteins. Therefore, one could predict that deletion of exon 6 would affect the transcriptional activity and nuclear localization of Glis2. To determine the effect of this deletion on Glis2 activity, the ability of Glis2^{mut} to repress GLI1-mediated transcriptional activation of a Luc reporter was examined in HEK293. In contrast to full-length Glis2, Glis2^{mut} was unable to repress the induction of GBS-dependent transcription of a Luc reporter by GLI1 as it was unable to compete with GLI1 for GBS binding (Fig. 1C). In addition to impaired transcriptional activity, this deletion also affected the nuclear localization of Glis2. In contrast to full-length Glis2, which is predominantly localized to the nucleus (Fig. 1D), Glis2^{mut} is equally distributed between the nucleus and cytoplasm, consistent with previous observations (47). These data indicate that Glis2^{mut} is unable to mediate GBS-dependent transcriptional regulation. Thus, the Glis2^{mut} mice generated are defective in this Glis2 function.

Glis2^{mut} mice develop progressive chronic kidney disease. Crossbreeding of Glis2 heterozygous mice produced litters with all three genotypes with the expected Mendelian distribution. Glis2^{mut} mice had a normal appearance and exhibited normal body weights and sizes. In addition, no behavioral or motor coordination abnormalities were observed. The Glis2^{mut} mice appeared healthy during the early stages of life. However, Glis2^{mut} mice exhibited significantly shorter life spans than did WT mice (Fig. 2A). At 10 months after birth, more than 40% of the Glis2^{mut} mice had died, while over the same time period, more than 95% of WT mice survived. Heterozygous mice exhibited normal life spans (data not shown).

Histopathological examination of a wide variety of tissues, including brain, liver, spleen, and lung, did not reveal any significant morphological/structural abnormalities except for in the kidney. No differences in kidney weight or size were observed between newborn WT and Glis2^{mut} mice (data not shown). At postnatal day 10 (PND10), the kidneys of WT and

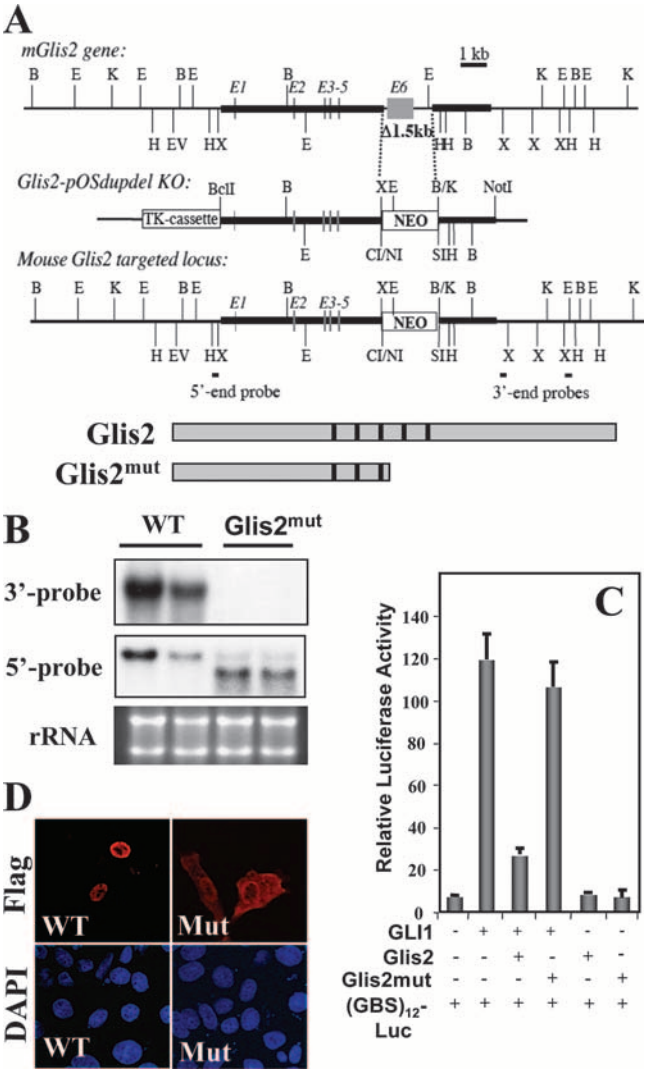

FIG. 1. Targeting the Glis2 locus. (A) Schematic view of the mouse Glis2 locus, the targeting vector pOSdupdel-Glis2, and the recombination at the Glis2 locus. In the targeted locus, a 1.5-kb region encoding the entire exon 6 is deleted. Gray bars indicate exons E1 to E6. The Glis2 and Glis2^{mut} proteins are schematically shown below the target locus. Black bars indicate zinc finger motifs. (B) Expression of Glis2 mRNA. Northern blot analysis was performed with RNA from kidneys of WT and homozygous mice by using a radiolabeled 3′ or 5′ Glis2 cDNA probe. (C) Effect of the C-terminal deletion on Glis2 transcriptional activity. The repression by Flag-Glis2 and Flag-Glis2^{mut} on GBS-dependent transactivation of a luciferase reporter (GBS_{12}-LUC) by GLI1 was examined in HEK293 cells. Error bars indicate standard deviations. −, absence of; +, presence of. (D) Flag-Glis2 (WT) and Flag-Glis2^{mut} (Mut) were expressed in HEK293 cells and their subcellular localization was examined by confocal microscopy with an anti-Flag and anti-mouse Alexa 595 antibody. Nuclei were stained with DAPI (4′,6′-diamidino-2-phenylindole).

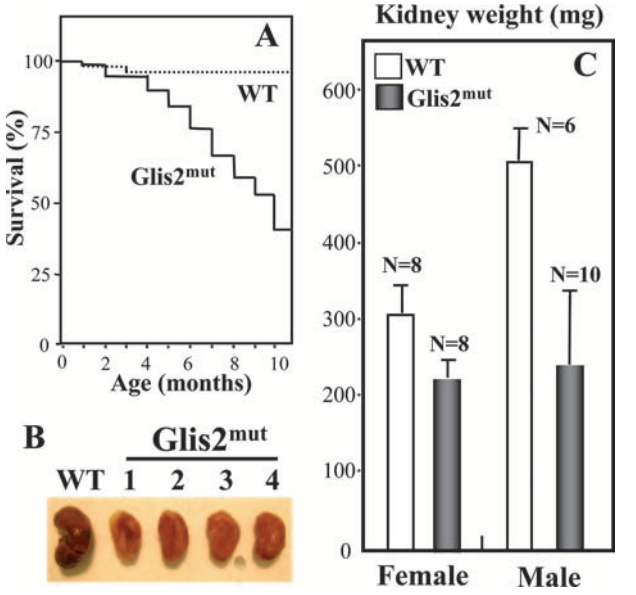

FIG. 2. Glis2^{mut} mice exhibit reduced life spans and kidney sizes. (A) The survival of WT (n = 29) and Glis2^{mut} mice (n = 43) was monitored over an 11-month period. The percentage of surviving mice was calculated. (B) Glis2^{mut} mice exhibited reduced kidney sizes. Kidneys typical for 6-month-old male WT and Glis2^{mut} mice are shown. (C) The average weight of kidneys from 6-month-old male and female WT and Glis2^{mut} mice was determined. Error bars indicate standard deviations.

Glis2^{mut} mice were histologically indistinguishable, suggesting that Glis2 deficiency did not significantly affect kidney organogenesis during embryonic development. In contrast, the kidneys of adult Glis2^{mut} mice were generally smaller and often paler than those of WT mice (Fig. 2B and C) and, in some cases, exhibited irregular surfaces. Kidneys became smaller and progressively atrophic with age (Fig. 3A). To determine whether this involved increased cell death, kidney sections of WT and Glis2^{mut} mice were examined by immunohistochemistry with an antibody against active caspase 3, a marker of apoptosis (12). A significant number of caspase 3-positive cells were detectable throughout the kidney sections from Glis2^{mut} mice, while only few caspase 3-positive cells were detectable in sections of WT kidneys (Fig. 3B and C). Increased cell death in Glis2^{mut} kidneys was supported by increased terminal deoxynucleotidyltransferase-mediated dUTP-biotin nick end labeling (TUNEL) staining throughout the kidney (data not shown). Quantitation of the number of TUNEL-positive cells revealed that renal tubules of Glis2^{mut} kidneys exhibited a number of TUNEL-positive cells fivefold higher than that of WT kidneys (Fig. 3C). Thus, the observed renal atrophy appears to be at least in part due to increased apoptosis.

Histopathological evaluation indicated that Glis2^{mut} mice developed progressive chronic kidney disease comprised of a spectrum of lesions that increased in severity and extent as the animals aged. Kidneys from heterozygous mice were indistinguishable from those of WT mice, suggesting that the Glis2^{mut} mutation results in a recessive phenotype. A significant feature of this phenotype was that the progression of the lesions was variable, and component lesions with various levels of severity were observed in animals of the same age or age range. No significant differences were detected between males and females in the progression or severity of nephropathy, and WT mice generally did not develop progressive nephropathy. The earliest lesions became apparent in proximal tubules and glomeruli of the outer cortices of Glis2^{mut} mice by PND25. The lesions were focal, involving few widely scattered, small clusters of cortical tubules and individual glomeruli. In contrast to

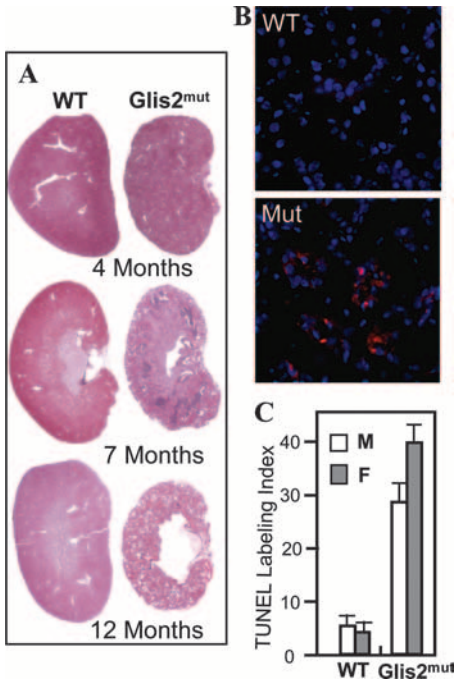

FIG. 3. Progressive degeneration and increased cell death in kidneys of Glis2^{mut} mice. (A) Representative H&E-stained sections of whole kidneys from 4-, 7-, and 10-month-old WT and Glis2^{mut} mice (same magnification). (B) Increased apoptosis in kidneys of Glis2^{mut} mice. Sections of kidneys from 10-month-old WT and Glis2^{mut} (Mut) mice were examined by immunohistochemistry with an anti-active-caspase 3 antibody as described in Materials and Methods. Nuclei were identified by DAPI (4′,6′-diamidino-2-phenylindole) staining. (C) Increased cell death in renal tubules. Kidney sections from 8-month-old male (M) ($n = 4$) and female (F) ($n = 7$) WT, and male ($n = 9$) and female ($n = 7$) Glis2^{mut} mice were stained by TUNEL, and the average number of TUNEL-positive cells associated with renal tubules in 10 random sections (TUNEL labeling index) was determined. Error bars indicate standard deviations.

normal tubules (Fig. 4A), affected tubules were smaller (atrophic) and lined by basophilic epithelial cells (Fig. 4B). Additionally, there was minimal thickening of the basement membranes of the initial segment of proximal convoluted tubules, as they originate from the glomeruli and the capsule (Bowman's capsule) surrounding glomeruli (Fig. 4C and D).

By 3 to 4 months, the lesions were more frequent in the cortex and may be associated with mild interstitial mononuclear inflammatory (primarily lymphocytic) cell infiltrates with associated subtle interstitial fibrosis (Fig. 4E and F). With further progression, the above-mentioned lesions were more prominent, frequent and consistently present in the cortex and increasingly involved the inner cortex and outer medulla. By 5 to 8 months of age, mononuclear inflammatory cell infiltrates were more extensive and especially prominent around the vasculature large perivascular infiltrates in the renal cortex of Glis2^{mut} mice (Fig. 4G and H). In addition, the glomerular Bowman's space and some cortical and medullary tubules were dilated and some tubules contained protein (data not shown).

By 8 to 12 months of age, the changes in the cortex were moderately to markedly severe and chronic in nature and involved the majority of the cortex (Fig. 4I to L). Tubules were variably dilated and many contained protein. Chronic glomerular changes included variable atrophy, glomerulosclerosis, thickening of the basement membrane of Bowman's capsule, and more pronounced dilatation of Bowman's spaces (see Fig. S2 the supplemental material for a large image). Mononuclear interstitial infiltrates and fibrosis were consistent and prominent features. Immunohistochemical staining with Pax5, CD3, and F4/80 antibodies identified these cells as a mixture of largely T and B lymphocytes and macrophages, respectively (Fig. 5). Infiltration of inflammatory cells was not observed in other tissues of Glis2^{mut} mice, and spleens remained normal. The development of extensive interstitial fibrosis was supported by an increase in collagen deposits, as indicated by enhanced staining with an anti-collagen I antibody (Fig. 5E and F) and Masson's trichrome (see Fig. S3 in the supplemental material).

Development of proteinuria in Glis2^{mut} mice. Close observation of the Glis2^{mut} mice showed increased water consumption and urine output supporting the development of impaired renal function in these mice (Fig. 6A). The latter was substantiated by the development of significant proteinuria in Glis2^{mut} mice (Fig. 6B). Only major urinary proteins were detectable in the urine samples of 10-month-old WT mice. In contrast, the urine samples of Glis2^{mut} mice contained many additional proteins; several of the major proteins were identified by mass spectrometry as transferrin, albumin, and the protease inhibitor serpine (Fig. 6B). At 1 year of age, 35% of the Glis2^{mut} mice had developed proteinuria, while only 10% of the WT mice had done so (Table 1). These numbers did not take into account the Glis2^{mut} mice that developed proteinuria and died of renal failure at an earlier age. The development of progressive renal disease in Glis2^{mut} mice was supported by increased levels of BUN and creatinine in serum. In most WT mice that were 10 months old or younger, the levels of blood BUN and creatinine remained below 30 mg/ml and 0.3 mg/ml, respectively (Fig. 6C and D), whereas Glis2^{mut} mice as young as 3 months old exhibited elevated levels of BUN and creatinine. These levels increased steadily with age in Glis2^{mut} mice. Mice with high BUN and creatinine levels frequently died of renal failure or had to be euthanized shortly after the time the analysis was performed. No evidence was found indicating that the renal phenotype of Glis2^{mut} mice involved diabetic or immunoglobulin A nephropathy or an autoimmune response, since no significant differences were observed in blood glucose levels, immunoglobulin A staining, serum immunoglobulin isotyping, or the level of anti-double-stranded DNA autoantibodies between 10-month-old WT and Glis2^{mut} mice (data not shown).

Changes in gene expression in kidneys from Glis2^{mut} mice. Because Glis2 functions as a regulator of transcription (21, 47), we were interested in examining what alterations in gene expression were associated with the early histopathological changes in Glis2^{mut} mice. Microarray analysis was performed to determine the gene expression profiles of kidneys from PND25 and PND60 WT and Glis2^{mut} mice. A comparison of the gene expression profiles identified a number of changes in gene expression in kidneys of Glis2^{mut} mice (see Table S2 in the supplemental material). An analysis of the gene expression profiles showed that about 336 genes were induced or repressed by 2.0-fold or more in the kidneys of PND60 Glis2^{mut} mice compared to those of WT mice. Of these genes, about

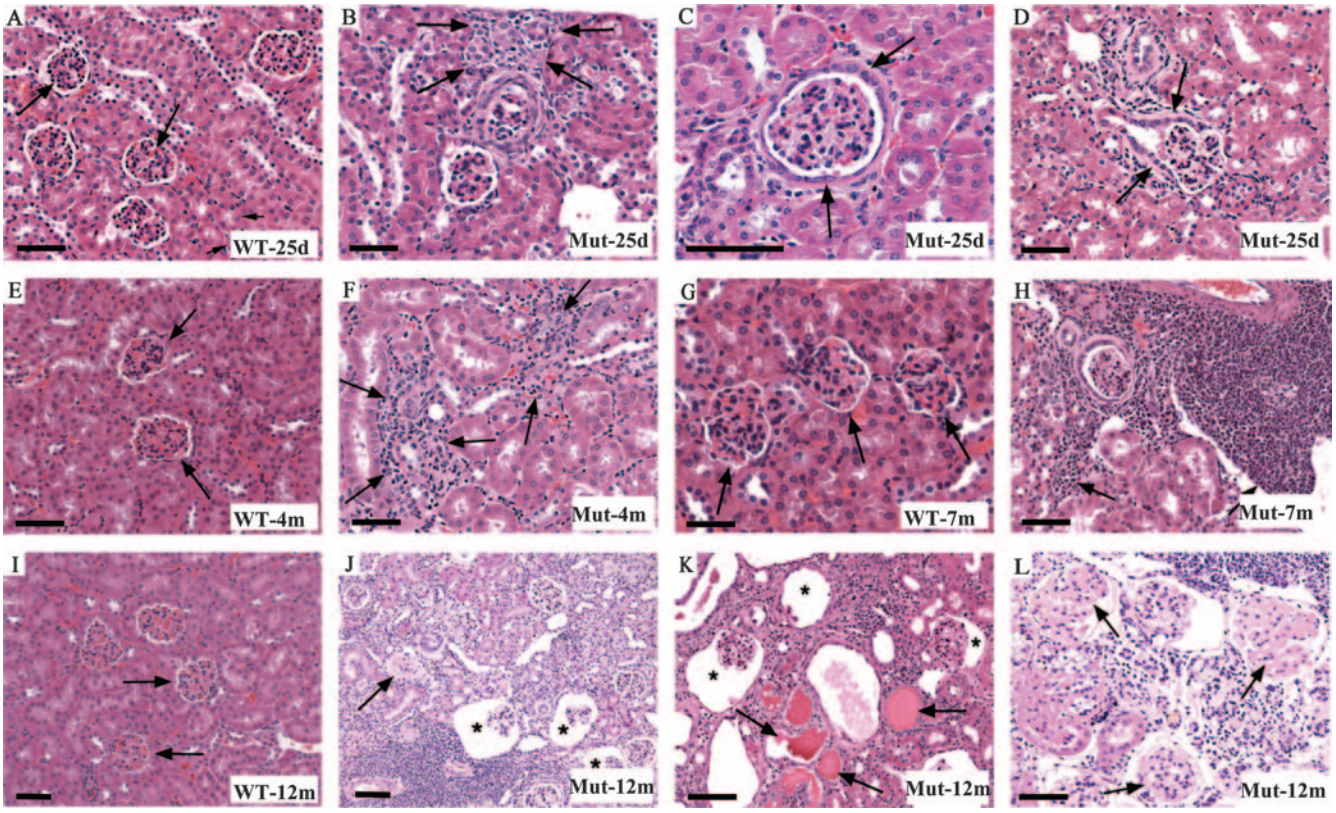

FIG. 4. Glis2^{mut} mice develop chronic kidney disease. (A) Kidney cortex from a PND25 WT mouse (WT-25d) showing normal glomeruli (long arrows) and proximal tubules (short arrows). (B to D) Representative sections of kidney from a PND25 Glis2^{mut} mouse (Mut-25d) illustrating early lesions in the cortex. (B) Focal cluster of atrophic proximal tubules lined by cuboidal, basophilic epithelial cells (arrows). Minimal thickening of the basement membrane of Bowman's capsule (C) and of the initial segment of a proximal tubule as it originates from the glomerulus (arrows) (D). (E) Kidney cortex from a 4-month-old WT mouse (WT-4m) showing normal glomeruli (arrows) surrounded by normal tubules. (F) Representative section of kidney from a 4-month-old Glis2^{mut} mouse (Mut-4m) with minimal to mild mononuclear cell infiltrates (arrows) within the interstitium. (G) Kidney cortex from a 7-month-old WT mouse (WT-7m) showing normal glomeruli (arrows) surrounded by normal tubules. (H) Representative section of kidney from a 7-month-old Glis2^{mut} mouse (Mut-7m) with more severe mononuclear cell infiltrates (arrows) within the interstitium. (I) Kidney cortex from a 12-month-old WT mouse (WT-12m) showing normal glomeruli (arrows) surrounded by normal tubules. (J to L) Representative sections of kidney from 12-month-old Glis2^{mut} mice (Mut-12m) illustrating advanced cortical lesions with widespread interstitial fibrosis with lymphocytic infiltrates throughout the interstitium. In the areas of fibrosis, there is also atrophy and loss of the proximal tubules. Glomerular changes include dilatation of the Bowman's space with atrophy of the capillary tuft (asterisk), thickening of the basement membrane of Bowman's capsule, and glomerular sclerosis (arrow). (K) Advanced lesion in the kidney showing a group of dilated tubules, several of which contain protein (arrows). Also note the glomeruli with dilated Bowman's space and atrophic capillary tufts (asterisk) and interstitial fibrosis with lymphocytic infiltrates. (L) Glomeruli with advanced glomerulosclerosis. All images are H&E-stained sections. Scale bars, 50 μm.

17% (55 genes) were down-regulated in kidneys of PND60 Glis2^{mut} mice, while 83% (278 genes) were induced. The large percentage of up-regulated genes fits the concept that Glis2 functions as a transcriptional repressor (21, 47). Microarray analysis using kidneys from PND25 mice identified many of the same changes in gene expression as observed with PND60 mice (see Table S2 in the supplemental material). Interestingly, many of the genes that were most significantly up-regulated in the PND60 kidneys of Glis2^{mut} mice encoded proteins involved in immune/inflammatory responses or in extracellular matrix (ECM) homeostasis. These included genes encoding the inflammatory chemokines Cxcl10 (IP10), Ccl5 (RANTES), Cx3cl1 (fractalkine), and Ccl2 (monocyte chemoattractant protein 1), the complement components C3 and C1q, and the adhesion proteins Vcam1 and Icam1. Up-regulated genes implicated in ECM homeostasis and fibrosis included the matrix gla protein (Mgp), the protease inhibitor plasminogen activator inhibitor type 1 (PAI-1), latent transforming growth factor β (TGF-β) binding protein 2 (Ltbp2), matrix metalloproteinase 14 (MMP14), connective tissue growth factor (Ctgf), vimentin, the calcium binding protein S100A4 (FSP1), and several procollagen genes, particularly procollagens 1α2 and 3α1. The induction of genes with established roles in renal fibrosis is in agreement with the development of glomerulosclerosis and interstitial fibrosis observed in kidneys from Glis2^{mut} mice.

Only 17% of the genes that were changed twofold or more were down-regulated in kidneys of Glis2^{mut} mice. These included the bifunctional apoptosis regulator (Bfar), insulin-like growth factor 2 (Igf2), and disrupted in renal carcinoma 2 (Dirc2) genes (see Table S2 in the supplemental material). Bfar is an intracellular membrane protein that regulates apoptosis by interacting with Bcl-2, Bcl-X(L), and death effector domain-containing procaspases (48). The Dirc2 gene encodes a member of the major facilitator superfamily of transporters

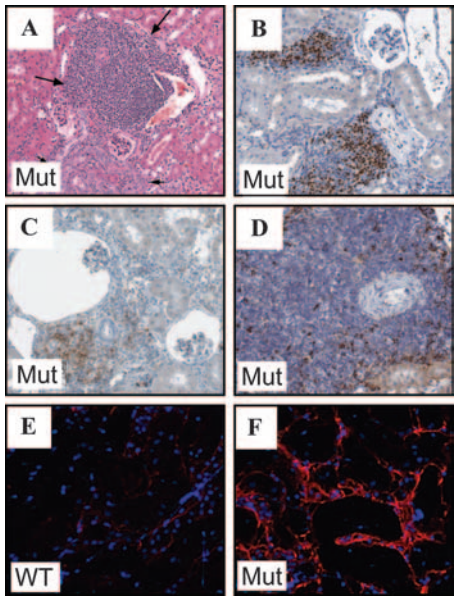

FIG. 5. Massive infiltration of T and B lymphocytes and macrophages and fibrosis in kidneys of Glis2^{mut} mice. (A) Infiltration of inflammatory cells (H&E staining) in kidney of a 10-month-old Glis2^{mut} mouse. Histochemical staining of sections of kidney from 10-month-old Glis2^{mut} mice for Pax5, a marker for B lymphocytes (B); CD3, a marker for T lymphocytes (C); and F4/80, a marker for macrophages (D). Immunofluorescence staining of representative sections of kidneys from WT (E) and Glis2^{mut} mice (F) with an anti-collagen I antibody and Alexa Fluor 594.

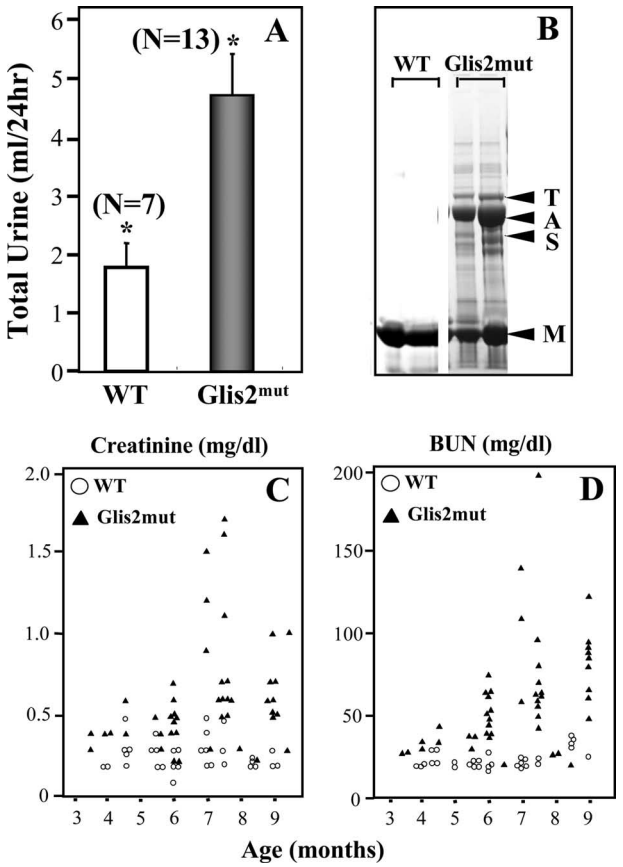

FIG. 6. Glis2^{mut} mice develop proteinuria and impaired renal functions. (A) Glis2^{mut} mice exhibit increased urine output. Urine output was measured in 12-month-old WT and Glis2^{mut} mice over a 24-h period. Error bars indicate standard deviations. Asterisks indicate $P < 0.01$. (B) Urine proteins of WT and Glis2^{mut} mice were analyzed by polyacrylamide gel electrophoresis. After Coomassie brilliant blue staining, several proteins were identified by matrix-assisted laser desorption ionization mass spectrometry. T, transferrin; A, albumin; S, serpine; M, major urinary proteins. (C and D) Levels of creatinine and BUN in WT and Glis2^{mut} mice were monitored over a period of 3 to 10 months. Glis2^{mut} mice exhibit significantly elevated blood levels of BUN and creatinine.

and a breakpoint targeting Dirc2 at chromosome 3q21 is associated with a significantly increased predisposition for renal cell cancer in humans (4). These proteins may potentially have an important function in the development of the renal pathology and apoptosis observed in Glis2^{mut} mice.

Real-time QRT-PCR analyses. Real-time QRT-PCR analysis was performed to validate the differential expression of a number of genes between kidneys of PND25 WT and Glis2^{mut} mice. Figure 7A shows that the expression of Ltbp2, Cxcl10, Ccl2, Col1a1, Mgp, gamma interferon, C3, PAI-1, TGF-β1, and Sparc were all enhanced severalfold and supports the data obtained by microarray analysis. To examine the correlation between the induction of these genes and renal phenotype, the expression of several genes was analyzed in mice of different ages. The expression of Ccl2, Ccl10, Mgp, and Ltbp2 increased with the age of Glis2^{mut} mice (Fig. 7B). For most genes, no significant change in expression was observed between kidneys from PND10 WT and Glis2^{mut} mice. This result is consistent with the observation that no obvious histological differences were noticed between these kidneys. Increased PAI-1 and Vcam-1 expression was confirmed by Western blot analysis (see Fig. S4 in the supplemental material).

DISCUSSION

To obtain greater insight into the physiological role of Glis2 (46, 47), we generated mutant mice deficient in the expression of Glis2. Histopathological analysis of kidneys from Glis2^{mut} mice revealed that Glis2^{mut} mice developed progressive chronic kidney disease that became more severe with age. The renal phenotype was characterized by tubular atrophy, interstitial fibrosis, glomerulosclerosis, pronounced dilatation of Bowman's spaces and tubules, and extensive infiltration of inflammatory cells. In addition, levels of BUN and creatinine increased and Glis2^{mut} mice developed proteinuria. These conditions ultimately resulted in renal failure and premature death of Glis2^{mut} mice. The progressive renal atrophy appears to be

TABLE 1. Enhanced development of proteinuria in Glis2 mice[a]

Mouse strain	No. of mice with protein concentration of:	
	<30 mg/ml	>150 mg/ml[b]
Glis2$^{+/+}$	9	1 (10)
Glis2^{mut}	15	8 (35)

[a] One-year-old mice were tested for proteinuria.
[b] Numbers in parentheses indicate percentages of the total number of mice with proteinuria.

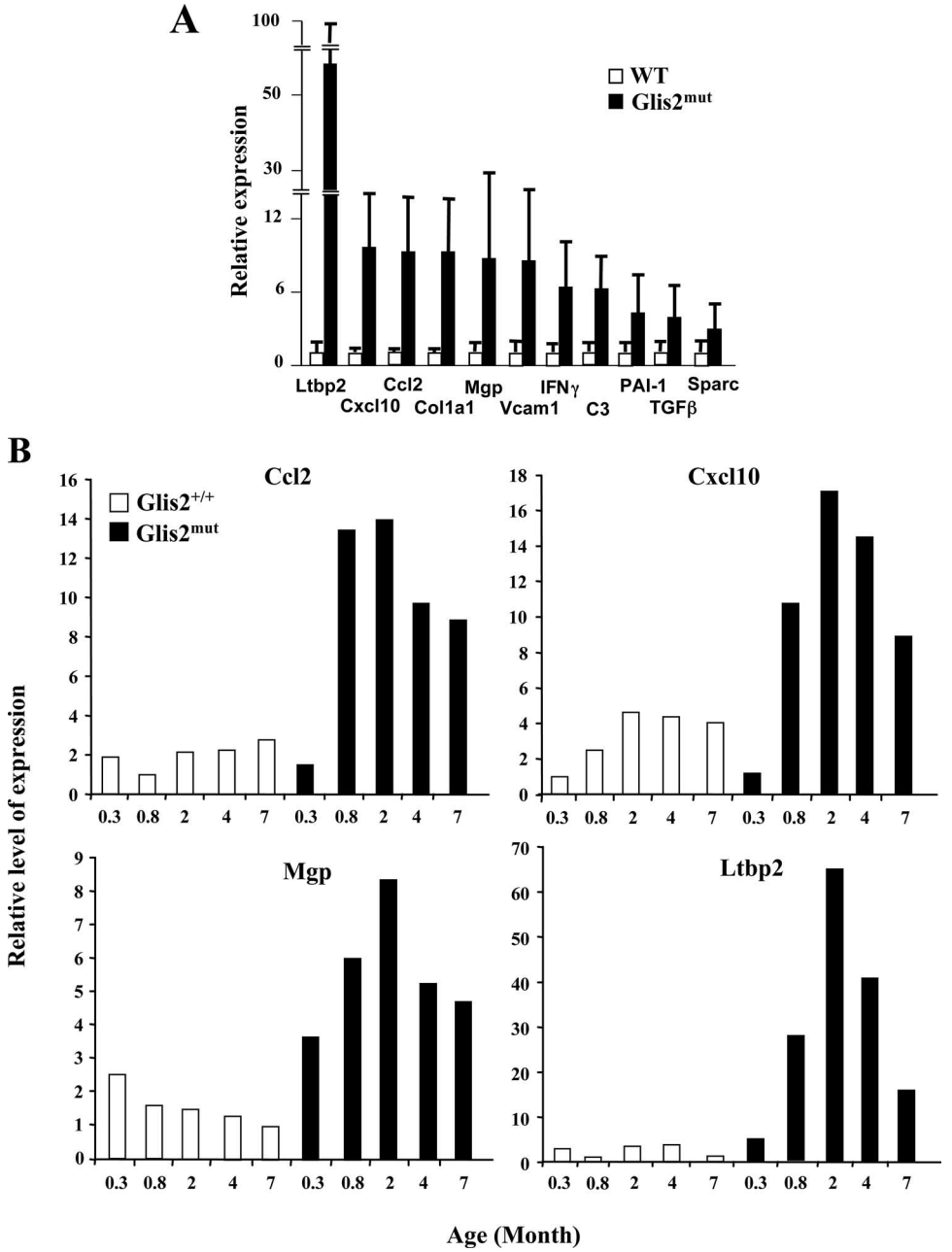

FIG. 7. Increased expression of genes involved in immune/inflammatory responses and ECM homeostasis in kidneys from Glis2^{mut} mice. (A) RNA was isolated from kidneys of WT and Glis2^{mut} mice. The level of expression of the genes indicated was analyzed by QRT-PCR in five individual samples. The increase in mRNA expression in kidneys from Glis2^{mut} mice was calculated and plotted. Error bars indicate standard deviations. (B) Expression levels of Ccl2, Cxcl10, Mgp, and Ltbp2 mRNA in kidneys from WT and Glis2^{mut} mice in relation the age of the mice. RNA from five mice in each group were pooled and analyzed by QRT-PCR. IFN-γ, gamma interferon.

at least in part related to increased apoptosis of tubule epithelial cells and other cells and may explain the reduction in kidney size during aging. The renal abnormalities observed in mice defective in Glis2 function resemble those associated with nephronophthisis, an autosomal recessive chronic kidney disease that is the most frequent genetic cause of end-stage renal failure (2, 14; this study). The loss of GLIS2, due to a change in the first nucleotide of the 5th intron of the GLIS2 gene that destroys this splice site, has recently been linked to nephronophthisis (2). The result of this mutation is similar to that of the mutation generated in our Glis2 mutant mice that lack the entire exon 6 region. Common features between the Glis2^{mut} phenotype and nephronophthisis include a loss of kidney size, tubular atrophy, severe chronic fibrosis, and the development of renal failure during early stages of life. As with nephronophthisis, the Glis2^{mut} mutation is recessive in nature since heterozygous mice have a normal phenotype. These observations suggest that Glis2 plays a critical role in maintaining

normal kidney architecture and functions and are in agreement with findings showing that a lack of GLIS2 expression results in the development of nephronophthisis (2).

The histopathological observations showed that fibrosis is a prominent feature of the renal phenotype in Glis2^{mut} mice. Progressive fibrosis often leads to organ failure in several tissues, including lung, kidney, liver, and heart. The pathogenic mechanisms that lead to chronic kidney disease converge on a common pathway that results in progressive interstitial fibrosis and dysfunctioning nephrons due to tubular atrophy (9, 26, 30). This appears to be an important cause of the renal failure and premature death in Glis2^{mut} mice. Tubulointerstitial fibrosis involves significant changes in normal renal architecture. It is characterized by an accumulation of ECM components and a thickening of the basement membrane and is related to a disturbance of the delicate balance between ECM degradation and synthesis (7, 9, 18, 29, 30, 36, 38, 42–45). A comparison of the gene expression profiles of kidneys from WT and Glis2^{mut} mice shows that the development of fibrosis in Glis2^{mut} mice is accompanied by increased synthesis of various ECM components, such as various types of collagen, Ltbp2, and vimentin, and by changes in the synthesis of enzymes that catalyze the degradation of ECM, including PAI-1. Much of the matrix deposition is believed to be synthesized by myofibroblasts. The increase in the number of myofibroblasts during renal fibrosis may occur by several mechanisms, including myofibroblast transdifferentiation (MFT), tubular epithelial-mesenchymal transition (EMT), and the infiltration of fibrocytes (9, 18, 29, 30, 36, 38, 42–45). Fibrosis often involves a combination of these processes. MFT, in which mesangial cells, fibrocytes, or fibroblasts transdifferentiate into myofibroblasts, can be involved in glomerulosclerosis and interstitial fibrosis. In EMT, tubular epithelial cells undergo transdifferentiation into myofibroblasts that then migrate into the interstitium. Each of these mechanisms might play a role in the renal phenotype observed in Glis2^{mut} mice. However, staining for Coll^{+}CD45^{+} fibrocytes did not show much difference between kidney sections of WT and Glis2^{mut} mice (unpublished observations), suggesting that the recruitment and infiltration of fibrocytes may not be a major feature of the renal phenotype observed in Glis2^{mut} mice.

A large number of cytokines and growth factors play critical roles in the regulation of ECM homeostasis (9, 30, 36, 39, 42). TGF-β1 particularly plays a major role in renal fibrosis and has been reported to promote EMT. The expression levels of TGF-β1 were increased in the kidneys of Glis2^{mut} mice, as were those of many TGF-β target genes, including PAI-1, Col1a, vimentin, S100A4 (FSP1), Ctgf, and Tgfbi (39). In addition, the expressions of the ECM proteins Ltbp2 and fibrillin 1 are induced in Glis2^{mut} mice. Many of these genes have been reported to be induced in activated (myo)fibroblasts. Moreover, all of these proteins play an important role in the control of ECM homeostasis and have been implicated in renal fibrosis. Ctgf induces collagen I expression and has been implicated in both glomerulosclerosis and tubulointerstitial fibrosis (11). PAI-1, an inhibitor of tissue and urokinase plasminogen activators, proteins that promote ECM degradation, plays a critical role in ECM homeostasis (10, 13, 17). Increased production of PAI-1 causes matrix accumulation and has been implicated in glomerulosclerosis and interstitial fibrosis. Ltbps and fibrillin play an important role in regulating the bioavailability of TGF-β. Increased expressions of PAI-1, vimentin, S100A4, and Col1a2 have been reported to be associated with the EMT (5, 17, 45). Our data are in agreement with the concept that activation of the EMT is part of the increased tubulointerstitial fibrosis observed in Glis2^{mut} mice. Loss of Glis2 may promote EMT. In this context, it is interesting to note that during metanephric development, Glis2 is most highly expressed in the ureteric bud, the inductor of mesenchymal-epithelial conversion during tubule formation (47). However, the loss of Glis2 function does not appear to affect this conversion, as the kidneys of PND10 Glis2^{mut} mice appear normal.

Since Glis2 regulates transcription by binding to GBS in the regulatory regions of target genes, one might predict that the renal phenotype observed in Glis2^{mut} mice is initiated by aberrant expression of specific Glis2 target genes. This aberrant expression likely induces a cascade of events that results in the induction of fibrosis, EMT, apoptosis, and renal degeneration. Many of the changes in gene expression profiles identified in this study might relate to the progression of this chronic kidney disease. Future studies have to identify the target genes involved in the initiation of this renal phenotype.

The renal phenotype in Glis2^{mut} mice is associated with a dramatic infiltration of inflammatory cells, mainly T and B lymphocytes, and macrophages. Many of the genes up-regulated in kidneys of Glis2^{mut} mice encode proteins with functions in immune responses/inflammation, including Cxcl14, Cxcl10, Ccl5, Cxcl4, Cxcl12, Ccl2, Ccl7, Ccl8, and Cx3cl1 (fractalkine), consistent with the observed inflammatory response in Glis2^{mut} kidneys. In progressive chronic kidney disease, inflammatory and fibrotic responses often converge and reinforce each other. Tubules, inflammatory cells, and myofibroblasts synthesize molecules that activate the fibrogenic and inflammatory cascades. Although the precise role of inflammatory cells in the induction of MFT and EMT has not been well investigated, it is well established that inflammatory cells can secrete a number of profibrotic cytokines which in turn can recruit and activate (myo)fibroblasts and fibrocytes (37, 40). Increased expression of profibrotic chemokines such as Ccl2 likely participates in the induction of renal fibrosis observed in Glis2^{mut} mice. Activation of the Cx3cl1/Cx3cr1 system has been implicated in renal fibrosis and in streptozotocin-induced diabetic nephropathy (8, 37, 40), while Ccl5 has been implicated in many renal diseases (27). Ccl5, Ccl2, and Cx3cl1 promote the recruitment of immune cells from the peripheral blood, and their induction may enhance the infiltration of inflammatory cells in the kidneys of Glis2^{mut} mice.

Glis2 is highly expressed in the collecting ducts and to a lower degree in the tubules, where it was found to localize to the cilium (2, 47). Glis2 is not expressed in the glomeruli, mesenchymal, or endothelial cells. These results suggest that the initial effects by Glis2 likely stem from changes in gene expression in tubule and collecting duct epithelial cells and that the changes observed in the glomeruli are a consequence rather than a cause. The association of Glis2 with the cilium suggests that Glis2 nuclear localization and activity might be regulated by an external signal. It is interesting to note that the association with cilia has also been reported for members of the related Gli subfamily of transcription factors that act downstream of the Sonic hedgehog (6). Recent studies have pro-

vided evidence for a link between Glis2 and the β-catenin and p120 catenin signaling pathways (15, 22). Future studies have to establish the exact links between cilium, catenin signaling, Glis2 activity, and Glis2-regulated gene transcription.

In summary, in this study, we describe the generation and characterization of Glis2^{mut} mice. We show that Glis2^{mut} mice have a complex renal phenotype that resembles that of nephronophthisis. Mutant mice develop progressive tubular atrophy, severe interstitial fibrosis, glomerulosclerosis, and infiltration of inflammatory cells. This progressive chronic kidney disease ultimately results in renal failure and premature death. Gene expression profiling analysis supports the dysregulation of ECM homeostasis and is consistent with the infiltration of inflammatory cells in Glis2^{mut} kidneys. Our study demonstrates that Glis2 plays a critical role in maintaining normal kidney architecture and function. Glis2^{mut} mice provide an excellent model for the study of the molecular events that play a role in the initiation and progression of nephronophthisis.

ACKNOWLEDGMENTS

We thank J. Williams for the matrix-assisted laser desorption ionization–mass spectrometry and Natasha Clayton for her assistance with the immunohistochemical analyses.

This research was supported by the Intramural Research Program of the NIEHS, NIH.

None of the authors have any conflicts of interest.

REFERENCES

1. **Aruga, J.** 2004. The role of Zic genes in neural development. Mol. Cell. Neurosci. **26:**205–221.
2. **Attanasio, M., N. H. Uhlenhaut, V. H. Sousa, F. O'Toole, J., E. Otto, K. Anlag, C. Klugmann, A. C. Treier, J. Helou, J. A. Sayer, D. Seelow, G. Nurnberg, C. Becker, A. E. Chudley, P. Nurnberg, F. Hildebrandt, and M. Treier.** 2007. Loss of GLIS2 causes nephronophthisis in humans and mice by increased apoptosis and fibrosis. Nat. Genet. **39:**1018–1024.

2a. **Beak, J. Y., et al.** Functional analysis of the zinc finger and activation domains of Glis3 and mutant Glis3(NDH1). Nucleic Acids Res., in press.

3. **Beak, J. Y., H. S. Kang, Y. S. Kim, and A. M. Jetten.** 2007. Kruppel-like zinc finger protein Glis3 promotes osteoblast differentiation by regulating FGF18 expression. J. Bone Miner. Res. **22:**1234–1244.
4. **Bodmer, D., M. Eleveld, E. Kater-Baats, I. Janssen, B. Janssen, M. Weterman, E. Schoenmakers, M. Nickerson, M. Linehan, B. Zbar, and A. G. van Kessel.** 2002. Disruption of a novel MFS transporter gene, DIRC2, by a familial renal cell carcinoma-associated t(2;3)(q35;q21). Hum. Mol. Genet. **11:**641–649.
5. **Burns, W. C., P. Kantharidis, and M. C. Thomas.** 2007. The role of tubular epithelial-mesenchymal transition in progressive kidney disease. Cells Tissues Organs **185:**222–231.
6. **Caspary, T., C. E. Larkins, and K. V. Anderson.** 2007. The graded response to Sonic hedgehog depends on cilia architecture. Dev. Cell **12:**767–778.
7. **Catania, J. M., G. Chen, and A. R. Parrish.** 2007. Role of matrix metalloproteinases in renal pathophysiologies. Am. J. Physiol. Renal Physiol. **292:** F905–F911.
8. **Cockwell, P., S. J. Chakravorty, J. Girdlestone, and C. O. Savage.** 2002. Fractalkine expression in human renal inflammation. J. Pathol. **196:**85–90.
9. **Eddy, A. A.** 2005. Progression in chronic kidney disease. Adv. Chronic Kidney Dis. **12:**353–365.
10. **Eddy, A. A., and A. B. Fogo.** 2006. Plasminogen activator inhibitor-1 in chronic kidney disease: evidence and mechanisms of action. J. Am. Soc. Nephrol. **17:**2999–3012.
11. **Eikmans, M., J. J. Baelde, E. de Heer, and J. A. Bruijn.** 2003. ECM homeostasis in renal diseases: a genomic approach. J. Pathol. **200:**526–536.
12. **Fickert, P., M. Trauner, A. Fuchsbichler, G. Zollner, M. Wagner, H. U. Marschall, K. Zatloukal, and H. Denk.** 2005. Oncosis represents the main type of cell death in mouse models of cholestasis. J. Hepatol. **42:**378–385.
13. **Fogo, A. B.** 2003. Renal fibrosis: not just PAI-1 in the sky. J. Clin. Investig. **112:**326–328.
14. **Hildebrandt, F., and W. Zhou.** 2007. Nephronophthisis-associated ciliopathies. J. Am. Soc. Nephrol. **18:**1855–1871.
15. **Hosking, C. R., F. Ulloa, C. Hogan, E. Ferber, A. Figueroa, K. Gevaert, W. Birchmeier, J. Briscoe, and Y. Fujita.** 2007. The transcriptional repressor Glis2 is a novel binding partner for p120 catenin. Mol. Biol. Cell **18:**1918–1927.
16. **Hu, M. C., R. Mo, S. Bhella, C. W. Wilson, P. T. Chuang, C. C. Hui, and N. D. Rosenblum.** 2006. GLI3-dependent transcriptional repression of Gli1, Gli2 and kidney patterning genes disrupts renal morphogenesis. Development **133:**569–578.
17. **Huang, Y., and N. A. Noble.** 2007. PAI-1 as a target in kidney disease. Curr. Drug Targets **8:**1007–1015.
18. **Iwano, M., and E. G. Neilson.** 2004. Mechanisms of tubulointerstitial fibrosis. Curr. Opin. Nephrol. Hypertens. **13:**279–284.
19. **Kang, H. S., J. Y. Beak, Y. S. Kim, R. M. Petrovich, J. B. Collins, S. F. Grissom, and A. M. Jetten.** 2006. NABP1, a novel RORgamma-regulated gene encoding a single-stranded nucleic-acid-binding protein. Biochem. J. **397:**89–99.
20. **Kasper, M., G. Regl, A. M. Frischauf, and F. Aberger.** 2006. GLI transcription factors: mediators of oncogenic hedgehog signalling. Eur. J. Cancer **42:**437–445.
21. **Kim, S. C., Y. S. Kim, and A. M. Jetten.** 2005. Kruppel-like zinc finger protein Gli-similar 2 (Glis2) represses transcription through interaction with C-terminal binding protein 1 (CtBP1). Nucleic Acids Res. **33:**6805–6815.
22. **Kim, Y. S., H. S. Kang, and A. M. Jetten.** 2007. The Kruppel-like zinc finger protein Glis2 functions as a negative modulator of the Wnt/beta-catenin signaling pathway. FEBS Lett. **581:**858–864.
23. **Kim, Y. S., M. Lewandoski, A. O. Perantoni, S. Kurebayashi, G. Nakanishi, and A. M. Jetten.** 2002. Identification of Glis1, a novel Gli-related, Kruppel-like zinc finger protein containing transactivation and repressor functions. J. Biol. Chem. **277:**30901–30913.
24. **Kim, Y. S., G. Nakanishi, M. Lewandoski, and A. M. Jetten.** 2003. GLIS3, a novel member of the GLIS subfamily of Kruppel-like zinc finger proteins with repressor and activation functions. Nucleic Acids Res. **31:**5513–5525.
25. **Kinzler, K. W., and B. Vogelstein.** 1990. The GLI gene encodes a nuclear protein which binds specific sequences in the human genome. Mol. Cell. Biol. **10:**634–642.
26. **Klahr, S.** 2001. Progression of chronic renal disease. Heart Dis. **3:**205–209.
27. **Krensky, A. M., and Y. T. Ahn.** 2007. Mechanisms of disease: regulation of RANTES (CCL5) in renal disease. Nat. Clin. Pract. Nephrol. **3:**164–170.
28. **Lamar, E., C. Kintner, and M. Goulding.** 2001. Identification of NKL, a novel Gli-Kruppel zinc-finger protein that promotes neuronal differentiation. Development **128:**1335–1346.
29. **Lee, J. M., S. Dedhar, R. Kalluri, and E. W. Thompson.** 2006. The epithelial-mesenchymal transition: new insights in signaling, development, and disease. J. Cell Biol. **172:**973–981.
30. **Liu, Y.** 2006. Renal fibrosis: new insights into the pathogenesis and therapeutics. Kidney Int. **69:**213–217.
31. **Lukashova-v Zangen, I., S. Kneitz, C. M. Monoranu, S. Rutkowski, B. Hinkes, G. H. Vince, B. Huang, and W. Roggendorf.** 2007. Ependymoma gene expression profiles associated with histological subtype, proliferation, and patient survival. Acta Neuropathol. **113:**325–337.
32. **Merzdorf, C. S.** 2007. Emerging roles for zic genes in early development. Dev. Dyn. **236:**922–940.
33. **Mizugishi, K., J. Aruga, K. Nakata, and K. Mikoshiba.** 2001. Molecular properties of Zic proteins as transcriptional regulators and their relationship to GLI proteins. J. Biol. Chem. **276:**2180–2188.
34. **Nakanishi, G., Y. S. Kim, T. Nakajima, and A. M. Jetten.** 2006. Regulatory role for Kruppel-like zinc-finger protein Gli-similar 1 (Glis1) in PMA-treated and psoriatic epidermis. J. Investig. Dermatol. **126:**49–60.
35. **Nakashima, M., N. Tanese, M. Ito, W. Auerbach, C. Bai, T. Furukawa, T. Toyono, A. Akamine, and A. L. Joyner.** 2002. A novel gene, GliH1, with homology to the Gli zinc finger domain not required for mouse development. Mech. Dev. **119:**21.

35a. **National Institutes of Health.** 1996. Guide for the care and use of laboratory animals. Publication no. 86-23. National Academy Press, Washington, DC.

36. **Neilson, E. G.** 2006. Mechanisms of disease: fibroblasts—a new look at an old problem. Nat. Clin. Pract. Nephrol. **2:**101–108.
37. **Panzer, U., O. M. Steinmetz, R. A. Stahl, and G. Wolf.** 2006. Kidney diseases and chemokines. Curr. Drug Targets **7:**65–80.
38. **Schnaper, H. W.** 2005. Renal fibrosis. Methods Mol. Med. **117:**45–68.
39. **Schnaper, H. W., T. Hayashida, S. C. Hubchak, and A. C. Poncelet.** 2003. TGF-beta signal transduction and mesangial cell fibrogenesis. Am. J. Physiol. Renal Physiol. **284:**F243–252.
40. **Segerer, S., and C. E. Alpers.** 2003. Chemokines and chemokine receptors in renal pathology. Curr. Opin. Nephrol. Hypertens. **12:**243–249.
41. **Senee, V., C. Chelala, S. Duchatelet, D. Feng, H. Blanc, J. C. Cossec, C. Charon, M. Nicolino, P. Boileau, D. R. Cavener, P. Bougneres, D. Taha, and C. Julier.** 2006. Mutations in GLIS3 are responsible for a rare syndrome with neonatal diabetes mellitus and congenital hypothyroidism. Nat. Genet. **38:** 682–687.
42. **Simonson, M. S.** 2007. Phenotypic transitions and fibrosis in diabetic nephropathy. Kidney Int. **71:**846–854.
43. **Wada, T., N. Sakai, K. Matsushima, and S. Kaneko.** 2007. Fibrocytes: a new insight into kidney fibrosis. Kidney Int. **72:**269–273.
44. **Yokoyama, H., T. Wada, and K. Furuichi.** 2003. Chemokines in renal fibrosis. Contrib. Nephrol. **139:**66–89.

45. **Zeisberg, M., and R. Kalluri.** 2004. The role of epithelial-to-mesenchymal transition in renal fibrosis. J. Mol. Med. **82:**175–181.
46. **Zhang, F., and A. M. Jetten.** 2001. Genomic structure of the gene encoding the human GLI-related, Kruppel-like zinc finger protein GLIS2. Gene **280:** 49–57.
47. **Zhang, F., G. Nakanishi, S. Kurebayashi, K. Yoshino, A. Perantoni, Y. S. Kim, and A. M. Jetten.** 2001. Characterization of Glis2, a novel gene encoding a Gli-related, Kruppel-like transcriptional factor with transactivation and repressor functions. Roles in kidney development and neurogenesis. J. Biol. Chem. **12:**10139–10149.
48. **Zhang, H., Q. Xu, S. Krajewski, M. Krajewska, Z. Xie, S. Fuess, S. Kitada, K. Pawlowski, A. Godzik, and J. C. Reed.** 2000. BAR: an apoptosis regulator at the intersection of caspases and Bcl-2 family proteins. Proc. Natl. Acad. Sci. USA **97:**2597–2602.